



A dual-pass variational data assimilation framework for estimating soil moisture profiles from AMSR-E microwave brightness temperature

Xiangjun Tian,^{1,2} Zhenghui Xie,^{1,2} Aiguo Dai,³ Chunxiang Shi,⁴ Binghao Jia,¹ Feng Chen,¹ and Kun Yang⁵

Received 12 August 2008; revised 8 June 2009; accepted 17 June 2009; published 21 August 2009.

[1] To overcome the difficulties in determining the optimal parameters needed for a radiative transfer model (RTM), which acts as the observational operator in a land data assimilation system, we have designed a dual-pass assimilation (DP-En4DVar) framework to optimize the model state (volumetric soil moisture content) and model parameters simultaneously using the gridded Advanced Microwave Scanning Radiometer–EOS (AMSR-E) satellite brightness temperature data. This algorithm embeds a dual-pass (the state assimilation pass and the parameter optimization pass) optimization technique based on an ensemble-based four-dimensional variational assimilation method and a shuffled complex evolution approach (SCE-UA). The SCE-UA method optimizes the parameters using observational information, thereby leading to improved simulations. The RTM is used to estimate brightness temperature from surface temperature and soil moisture. This algorithm is implemented differently in two phases: the parameter calibration phase and the pure assimilation phase. Both passes are applied in each assimilation time window during the parameter calibration phase. However, only the state assimilation pass is used in the pure assimilation phase after the parameters are determined during the parameter calibration phase. Several experiments conducted using this framework coupled partially with a land surface model (the NCAR CLM3) show that volumetric soil moisture content can be significantly improved to be comparable with in situ observations by assimilating only daily satellite brightness temperature. Furthermore, the improvement in surface soil moisture also propagates to lower layers where no observations are available.

Citation: Tian, X., Z. Xie, A. Dai, C. Shi, B. Jia, F. Chen, and K. Yang (2009), A dual-pass variational data assimilation framework for estimating soil moisture profiles from AMSR-E microwave brightness temperature, *J. Geophys. Res.*, 114, D16102, doi:10.1029/2008JD011600.

1. Introduction

[2] As a lower boundary condition for numerical weather and climate models, soil moisture is a crucial variable for many hydrologic and climate studies. It strongly influences the partitioning of surface available energy into sensible and latent heat fluxes and hence the evolution of the lower atmospheric conditions. Some studies [e.g., *Chahine*, 1992] show that soil moisture's effect on the atmosphere is secondary only to that of sea surface temperature (SST) on a global scale and even exceeds SST's effect over land. Accurate knowledge of spatial and temporal variations

of soil moisture is needed for weather predictions and climate studies.

[3] Estimates of soil moisture can be obtained from several sources: in situ measurements, land surface models and satellite remote sensing. In situ measurements may be most accurate for given locations; however, they are often insufficient to represent large spatial variations in soil moisture. Current state-of-the-art land surface models can capture many of the spatial and temporal variations in soil moisture, but model results generally contain mean biases and may deviate from the true soil moisture evolution because of uncertainties in model parameters, structures, and input forcing data. There have been large efforts to create estimates of soil moisture fields using land surface models forced with realistic precipitation and other atmospheric forcing data, such as the Global Soil Wetness Project (<http://grads.iges.org/gswp/>) [*Dirmeyer et al.*, 1999], the North America Land Data Assimilation System (NLDAS) [*Mitchell et al.*, 2004], Global Land Data Assimilation System (GLDAS) (<http://ldas.gsfc.nasa.gov/>), and others [e.g., *Nijssen et al.*, 2001; *Qian et al.*, 2006; *Sheffield and Wood*, 2008].

¹ICCES, Institute of Atmospheric Physics, Chinese Academy of Sciences, Beijing, China.

²LASG, Institute of Atmospheric Physics, Chinese Academy of Sciences, Beijing, China.

³National Center for Atmospheric Research, Boulder, Colorado, USA.

⁴National Satellite Meteorological Center, China Meteorological Administration, Beijing, China.

⁵Institute of Tibetan Plateau Research, Chinese Academy of Sciences, Beijing, China.

[4] Low-frequency microwave brightness temperature seen by satellites is strongly affected by near-surface soil moisture content but not much by atmospheric states. Because of this, low-frequency microwave data have been used to retrieve soil moisture content [Jackson, 1993; Njoku and Entekhabi, 1996; Shi et al., 1997; Owe et al., 2001; Paloscia et al., 2001; Wigneron et al., 2003; Njoku et al., 2003; Wen et al., 2003; Zhang et al., 2006]. Unfortunately, remotely sensed soil moisture content still contains large errors and needs to be improved greatly. Another way to use the brightness temperature data is to assimilate them directly into a land surface model to improve modeling of soil moisture and thus the surface energy budget. Reichle et al. [2001] investigated the feasibility of estimating large-scale soil moisture profiles and related land surface variables from 1.4-GHz passive microwave measurements using variational data assimilation. Crow and Wood [2003] assessed the potential of assimilating surface brightness temperature data into a TOPMODEL-based land surface model using an ensemble Kalman filter (EnKF) method. Seuffert et al. [2003, 2004] also tested two different soil moisture systems based on a simplified extended Kalman filter (EKF) method and an optimal interpolation (OI) method using screen-level parameters and 1.4-GHz microwave brightness temperature. The two systems gave similar results compared to observed gravimetric soil moisture and surface heat fluxes. Recently, Yang et al. [2007a, 2007b] proposed a land surface assimilation system to assimilate Advanced Microwave Scanning Radiometer–EOS (AMSR-E) brightness temperatures of vertical polarization at 6.9 GHz and 18.7 GHz. However, only surface soil moisture is optimized in their assimilation system, which uses an iterative assimilation technique. Here we propose an assimilation framework that can improve the soil moisture profiles considerably by assimilating the gridded brightness temperature data, even though the satellite observations are only for the skin soil layer.

[5] How to fully use the microwave brightness temperature data for the top-few-centimeter soils to improve estimates of the soil moisture profiles is a difficult inverse problem. For some regions, this may not be achievable simply because surface soil moisture is not physically correlated with subsurface moisture content in these regions. For many other areas, land data assimilation provides an effective way to this problem by merging the information from remote sensing and models. In land data assimilation, Kalman filter methods, such as the extended Kalman filter (EKF) [Entekhabi et al., 1994] and ensemble Kalman filter (EnKF) [e.g., Evensen, 1994, 2003; Kalnay et al., 2007; Beezley and Mandel, 2008; Tian and Xie, 2008], are the most frequently used data assimilation algorithms. Different assimilation algorithms based on the EKF or EnKF method have been used to estimate soil moisture profiles using satellite observations of near-surface soil moisture content [Houser et al., 1998; Reichle et al., 2001; Crow and Wood, 2003; Reichle and Entekhabi, 2001; Reichle et al., 2002a, 2002b]. Among them, Entekhabi et al. [1994] first used the EKF technique to retrieve 1-m soil moisture profiles and compared them with other estimates. Walker et al. [2001] compared two assimilation schemes,

namely the direct insertion and EKF, in the context of retrieval rates. Reichle et al. [2002a] applied the EnKF to the retrieval problem of soil moisture distributions by assimilating synthetic surface brightness temperatures.

[6] On the other hand, the need for a linear version of the forecast model in the four-dimensional variational data assimilation (4DVar) method severely limits its application in soil moisture data assimilation because of the high nonlinearity in the soil water hydrodynamic equation [Reichle and Entekhabi, 2001; Reichle et al., 2002a, 2002b]. Recently, this issue was addressed by Tian et al. [2008a] using an ensemble-based explicit 4DVar method (referred to as En4DVar hereafter). Here, we design a dual-pass framework to optimize the soil moisture profile by assimilating AMSR-E microwave brightness temperature (T_b) data into a soil water hydrodynamic model. A radiative transfer model (RTM) is taken as the observational operator in this framework to provide a link between the forecast model and observational variables and to estimate T_b from surface temperature and soil moisture. The soil moisture profile is assimilated by the En4DVar method in the state assimilation pass. Simultaneously, several key parameters in the RTM are also optimized using the shuffled complex evolution approach (SCE-UA) from Duan et al. [1993] in the parameter optimization pass to account for their high variability or unavailability. This kind of dual-pass techniques have previously been implemented within the Kalman filter framework [Moradkhani et al., 2005a, 2005b; Vrugi et al., 2005; Tian and Xie, 2008; Tian et al., 2008b] and also in a variational system [Yang et al., 2007a, 2007b].

[7] Preliminary assimilation results show that soil moisture calculated through this dual-pass variational assimilation framework coupled partially with the Community Land Model version 3 (CLM3) [Oleson et al., 2004; Dickinson et al., 2006] is significantly improved to be comparable with in situ soil moisture observations by assimilating only daily satellite brightness temperatures. Moreover, the improvement is seen not only in the skin layer, but also, to a considerable extent, in lower layers where no observational data are available for assimilation. Thus, the whole soil moisture profile can be improved by assimilating microwave brightness temperatures of the top few centimeters. This provides a promising solution for soil moisture assimilation for uses in climate, hydrologic, and weather applications.

2. A Dual-Pass Variational Assimilation (DP-En4DVar) Framework

[8] The dual-pass assimilation framework consists of a soil water hydrodynamic model used in the CLM3 to calculate soil moisture, a radiative transfer model (RTM) to estimate microwave brightness temperature (T_b), and a dual-pass variational assimilation algorithm to simultaneously optimize the state variable and the parameters using brightness temperature data from satellite observations. This assimilation framework is somewhat similar to Yang et al. [2007a, 2007b]. However, they differ from each other significantly in two aspects: 1. The forecast operator used in our framework is 1-D soil water equation model used in

the NCAR Community Land Model (CLM) [Oleson *et al.*, 2004; Dickinson *et al.*, 2006], while a simple biosphere model (SIB2) [Sellers *et al.*, 1996] is adopted in Yang *et al.* [2007a, 2007b]; and 2. an ensemble-based explicit 4DVar method [Tian *et al.*, 2008a] is used to assimilate brightness temperature into soil moisture estimation in the assimilation pass in this study, whereas Yang *et al.* [2007a] used a variational assimilation approach based on an iterative technique in its assimilation procedure.

2.1. Soil Water Hydrodynamic Model

[9] The volumetric soil moisture (θ) for 1-D vertical water flow in a soil column in the CLM is expressed as

$$\frac{\partial \theta}{\partial t} = -\frac{\partial q}{\partial z} - E - R_{fm}, \quad (1)$$

where q is the vertical soil water flux, E is the roots' evapotranspiration rate, and R_{fm} is the melting (negative) or freezing (positive) rate, and z is the depth from the soil surface. Both q and z are positive downward.

[10] The soil water flux q is described by Darcy's law [Darcy, 1856]:

$$q = -k \frac{\partial(\phi + z)}{\partial z}, \quad (2)$$

where $k = k_s(\theta/\theta_s)^{2b+3}$ is the hydraulic conductivity, and $\phi = \phi_s(\theta/\theta_s)^{-b}$ is the soil matrix potential, k_s , ϕ_s , θ_s and b are constants. The CLM computes soil water content in the 10 soil layers through (1–2) (see Oleson *et al.* [2004] for details). The upper boundary condition is

$$q_0(t) = -k \frac{\partial(\phi + z)}{\partial z} \Big|_{z=0}, \quad (3a)$$

where $q_0(t)$ is the water flux at the land surface (referred to as infiltration), and the lower boundary condition is $q_l = 0$. The time step Δt is 1800 s (0.5 h).

2.2. Radiative Transfer Model

[11] Following Yang *et al.* [2007b], the microwave brightness temperature (T_b) can be estimated using

$$T_{b,p(q)} = T_g(1 - \Gamma_{p(q)}) \exp(-\tau_c) + T_c(1 - \omega)[1 - \exp(-\tau_c)] \times [1 + \Gamma_{p(q)} \exp(-\tau_c)], \quad (3b)$$

where the subscript $p(q)$ denotes vertical (horizontal) polarization, $\Gamma_{p(q)}$ is soil reflectivity, T_g is ground temperature, T_c is canopy temperature, τ_c is the optical thickness of the vegetation, and ω is the single-scattering albedo of the vegetation. The soil reflectivity can be calculated using a Q-h model [Wang and Choudhury, 1981] or a Q-p model [Shi *et al.*, 2005]; we use the Q-h model here. The soil reflectivity can be written as

$$\Gamma_{p(q)} = [(1 - Q) \cdot R_{p(q)} + Q \cdot R_{q(p)}] \exp(-h), \quad (4)$$

where Q and h are empirically determined surface roughness parameters, and R is the Fresnel power reflectivity that describes the soil reflectivity of a smooth surface.

[12] The vertical (R_p) and horizontal (R_q) Fresnel power reflectivities are calculated using

$$R_p = \left| \frac{\cos \theta - \sqrt{\varepsilon_r - \sin^2 \theta}}{\cos \theta + \sqrt{\varepsilon_r - \sin^2 \theta}} \right|^2 \quad (5a)$$

$$R_q = \left| \frac{\varepsilon_r \cos \theta - \sqrt{\varepsilon_r - \sin^2 \theta}}{\varepsilon_r \cos \theta + \sqrt{\varepsilon_r - \sin^2 \theta}} \right|^2, \quad (5b)$$

where θ is the incident angle and ε_r is the soil dielectric constant, which is calculated following Dobson *et al.* [1985]:

$$\varepsilon_r = \left[1 + (1 - w_s)(\varepsilon_s^\alpha - 1) + \omega^\beta \varepsilon_{fw}^\alpha - w \right]^{1/\alpha}, \quad (6)$$

where w_s is the soil porosity, w is the surface soil water content, $\varepsilon_s = (4.7, 0.0)$ is the dielectric constant of a very dry soil, ε_{fw} (≈ 81) is the dielectric constant of free water, $\alpha = 0.65$, and β is a soil texture-dependent coefficient [Ulaby *et al.*, 1986]:

$$\beta = 1.09 - 0.0011 \times P_s + 0.0018 \times P_c, \quad (7)$$

where P_s and P_c are the percentage of sand and clay in the soil, respectively.

[13] The model parameters in equations (3a), (3b) and (4) are frequency-dependent and are given by

$$h = (k \cdot S)^{\sqrt{0.1 \cos \theta}}, \quad (8)$$

$$Q = Q_0(k \cdot S)^{0.795}, \quad (9)$$

$$\tau_c = b'(100\lambda)^\chi w_c / \cos \theta, \quad (10)$$

$$\omega = 0.00083/\lambda, \quad (11)$$

where λ is the wavelength in meters, k is the wave number defined as $2\pi/\lambda$, S is the standard deviation of surface height, w_c is the vegetation water content in kg m^{-2} , and Q_0 , b' , and χ are empirical coefficients.

[14] Equation (8) follows Wegmuller and Matzler [1999], while equation (9) follows Jackson and Schmugge [1991] and equations (10) and (11) follow Yang *et al.* [2007b]. The value of χ depends on vegetation type (leaf dominated, stem-dominated, or grass), and Jackson and Schmugge [1991] suggest a value of -1.08 for stem-dominated and -1.38 for leaf dominated.

[15] The vegetation water content is estimated following Paloscia and Pampaloni [1988]:

$$w_c = \exp(\text{LAI}/3.3) - 1, \quad (12)$$

where LAI (in meters squared per meters squared) is the leaf area index.

[16] Given the needed parameters, the RTM estimates microwave brightness temperature (T_b) from the inputs of surface soil moisture content, ground temperature and canopy temperature. Several parameters (namely, S , Q_0 , and b') in the RTM significantly affect the outputs while their values are either highly variable or unavailable. How to obtain accurate values for parameters (S , Q_0 , b') is critical to the accuracy of the RTM's outputs and thus the performance of this variational assimilation framework. This issue is addressed further below.

2.3. Three Dual-Pass Variational Assimilation (DP-En4DVar) Algorithms

[17] Figure 1 shows the flowchart of our dual-pass assimilation algorithm, which embeds a dual-pass optimization technique. This algorithm is implemented differently in the parameter calibration phase and the pure assimilation phase. Both the state assimilation pass and the parameter optimization pass are used in the parameter calibration phase in each assimilation time window in order to obtain the optimal parameters for the RTM. However, only the state assimilation pass is used in the pure assimilation phase after the parameters are determined during the parameter calibration phase. Both passes assimilate observed brightness temperature of the vertical polarization at a lower (6.9 GHz) and a higher frequency (18.7 GHz). This is critical for producing stable and reliable estimates of soil moisture [Yang *et al.*, 2007b]. The vertical polarization is more desirable than the horizontal polarization because it is relatively insensitive to vegetation coverage [Fujii, 2005].

[18] Keeping all the parameters constant in the state assimilation pass, the soil moisture profile can be assimilated by the En4DVar method (see Tian *et al.* [2008a] for more details) using observed brightness temperature in each assimilation time window. In this method, as in the traditional implicit 4DVar analyses, the state variable \mathbf{x}_a (soil moisture content in this study) is obtained through the minimization of a cost function J that measures the misfit between the model trajectory $H_i(\mathbf{x}_i)$ and the observation \mathbf{y}_i at a series of times t_i , $i = 0, 1, \dots, m$:

$$J(\mathbf{x}_0) = (\mathbf{x}_0 - \mathbf{x}_b)^T B^{-1} (\mathbf{x}_0 - \mathbf{x}_b) + \sum_{i=0}^m [\mathbf{y}_i - H_i(\mathbf{x}_i)]^T \cdot R_i^{-1} [\mathbf{y}_i - H_i(\mathbf{x}_i)], \quad (13)$$

with the forecast model $M_{0 \rightarrow i}$ imposed as strong constraints, defined by

$$\mathbf{x}_i = M_{0 \rightarrow i}(\mathbf{x}_0), \quad (14)$$

where the superscript T stands for a transpose, \mathbf{x}_b is a background value, index i denotes the observational time, H_i is the observational operator, and matrices B and R are the background and observational error covariances, respectively. In our assimilation framework, the forecast model $M_{0 \rightarrow i}$ is the soil water hydrodynamic model (section 2.1) and the observational operator H_i is the RTM (section 2.2), respectively. The RTM actually establishes a mapping between the forecast state space (soil moisture content θ , calculated by the soil water hydrodynamic model)

and the observational variable space (observed brightness temperature, i.e., $\mathbf{y}_i = (T_{b,i}^{6.9V}, T_{b,i}^{18.7V})^T$ in (13)). The control variable is the initial conditions $\mathbf{x}_0(\theta(t_0))$ at the start of the assimilation time window of the model. In the cost function (13), the control variable \mathbf{x}_0 is connected with \mathbf{x}_i through forwarding the model (14) and expressed implicitly, which makes it difficult to compute the gradient of the cost function with respect to \mathbf{x}_0 . The following method, first proposed by Tian *et al.* [2008a], simplifies this problem.

[19] Assuming there are S time steps within the assimilation time window $(0, T)$. We first generate N random perturbation fields using the Monte Carol method and add each perturbation field to the initial background field at $t = t_0$ to produce N initial fields $\mathbf{x}_n(t_0)$, $n = 1, 2, \dots, N$. We then integrate the forecast model $\mathbf{x}_n(t_i) = M_i(\mathbf{x}_n(t_{i-1}))$ with the initial fields $\mathbf{x}_n(t_0)$ ($n = 1, 2, \dots, N$) throughout the assimilation time window to obtain the state series $\mathbf{x}_n(t_i)$ ($i = 0, 1, \dots, S - 1$) and then construct the perturbed 4-D fields (snapshots) \mathbf{X}_n ($n = 1, 2, \dots, N$) over the assimilation time window:

$$\mathbf{X}_n = (\mathbf{x}_n(t_0), \mathbf{x}_n(t_1), \dots, \mathbf{x}_n(t_{S-1})), n = 1, 2, \dots, N. \quad (15)$$

All the perturbed 4-D fields \mathbf{X}_n ($n = 1, 2, \dots, N$) can expand a finite ($\leq N$) dimensional space $\Omega(\overbrace{\mathbf{X}_1 \mathbf{X}_2 \dots \mathbf{X}_N})$. Similarly, the analysis field $\mathbf{x}_a(t_i)$ ($i = 0, 1, 2, \dots, S - 1$) over the same assimilation time window can also be stored into the following vector:

$$\mathbf{X}_a = (\mathbf{x}_a(t_0), \mathbf{x}_a(t_1), \dots, \mathbf{x}_a(t_{S-1})). \quad (16)$$

When the ensemble size N is increased by adding random samples, the ensemble space could cover the analysis vector \mathbf{X}_a , i.e., \mathbf{X}_a is approximately assumed to be in this linear space Ω . Then the analysis vector \mathbf{X}_a can be expressed by the linear combinations of the base vectors of the space Ω since it is in this space.

[20] How to obtain the appropriate base vectors remains the only task left. We found that the POD technique is a good choice for doing this. It can produce a set of base vectors spanning the ensemble of data in certain least squares optimal sense [Ly and Tran, 2001, 2002].

[21] We form N new ensemble members by focusing on deviations from the vector \mathbf{X}_i , ($i = 1, \dots, N$), respectively, as follows:

$$\delta \mathbf{X}_{ni} = \mathbf{X}_n - \mathbf{X}_i, \quad n = 1, \dots, N, \quad (17)$$

which form the matrixes A_i ($M \times N$).

[22] Using the proper orthogonal decomposition (POD) technique [e.g., Ly and Tran, 2001, 2002; S. Volkwein, unpublished manuscript, 2008] (available from <http://www.uni-graz.at/imawww/volkwein/publist.html>) to compute the POD models (base vectors, ϕ_j^i ($j = 1, \dots, P_i$)) of A_i , the truncated reconstruction of the analysis ensemble in the four dimensional space \mathbf{X}_a^i is given by

$$\mathbf{X}_a^i = \mathbf{X}_i + \sum_{j=1}^{P_i} \alpha_j^i \phi_j^i, \quad (18)$$

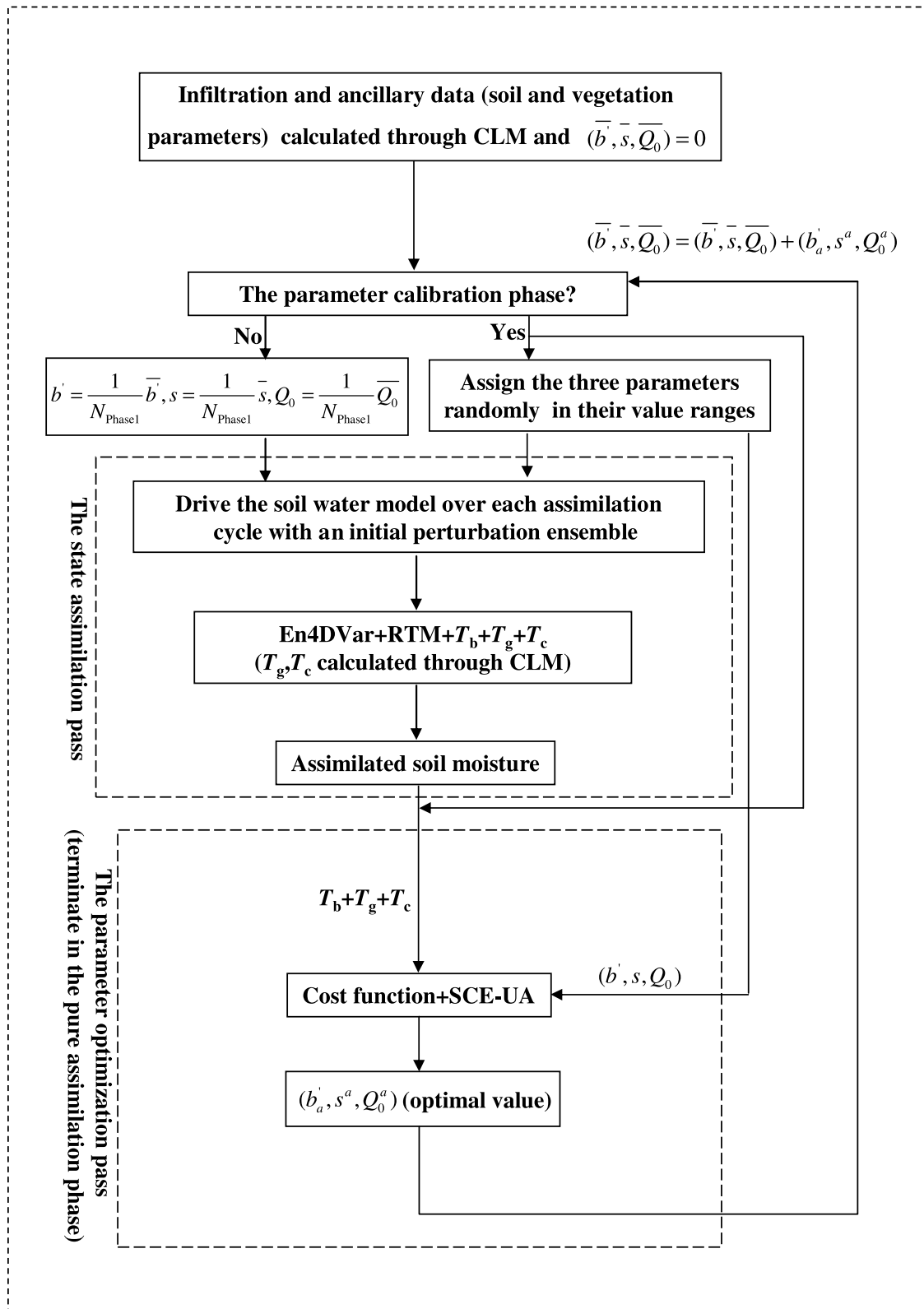


Figure 1. Algorithmic flowchart of the dual-pass variational assimilation framework.

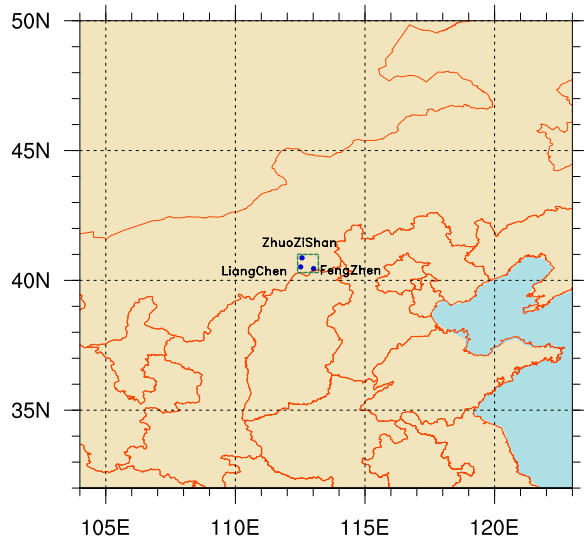


Figure 2. Map of the reference site. The grid of dashed lines is centered at (112.5°E, 40.5°N).

where P_i (the number of the POD modes of A_i) is defined by Tian *et al.* [2008a].

[23] Given the vector of measurements $Y = (\mathbf{y}_0, \mathbf{y}_1, \dots, \mathbf{y}_m)^T$, we can define the N vectors with perturbed observations as

$$Y_i = Y + E_i, i = 1, \dots, N, \quad (19)$$

where $E_i = (\varepsilon_{i,0}, \varepsilon_{i,1}, \dots, \varepsilon_{i,m})^T$ are random real vectors. The measurement error covariance matrix can be estimated using

$$R_j = \frac{E_j E_j^T}{N-1}, j = 0, \dots, m, \quad (20)$$

where $E_j = (\varepsilon_{1,j}, \dots, \varepsilon_{N,j})$.

[24] The cost function (13) can now be reformulated as follows:

$$J_i(\mathbf{x}_0) = (\mathbf{x}_0 - \mathbf{x}_b) B^{-1} (\mathbf{x}_0 - \mathbf{x}_b) + \sum_{j=0}^m \left[\mathbf{y}_{ji} - H_j(\mathbf{x}_j) \right]^T \cdot R_j^{-1} \left[\mathbf{y}_{ji} - H_j(\mathbf{x}_j) \right], \quad (21)$$

where $Y_i = (\mathbf{y}_{0i}, \dots, \mathbf{y}_{mi})$.

Substituting (18) into (21), the control variable becomes $\alpha_i = (\alpha_i^1, \dots, \alpha_i^{P_i})^T$ instead of $\mathbf{x}(t_0)$ and then the analysis ensemble $\bar{\mathbf{X}}_a^i$ ($i = 1, \dots, N$) can be easily obtained. The mean analysis state is then generated as follows:

$$\mathbf{X}_a = \frac{1}{N} \sum_{i=1}^N \mathbf{X}_a^i. \quad (22)$$

The ensemble initial A_0 for the next assimilation cycle is constructed by

$$A_0 = (\mathbf{x}_a^1(t_{S-1}), \dots, \mathbf{x}_a^N(t_{S-1})), \quad (23)$$

and the background error covariance B can be updated by the evolving analysis ensemble forecasts (so it is flow-dependent), as follows:

$$B = \frac{\Delta A_0 (\Delta A_0)^T}{N-1}, \quad (24)$$

where $\mathbf{x}_a^*(t_{S-1}) = \frac{1}{N} \sum_{n=1}^N \mathbf{x}_a^n(t_{S-1})$ and $\Delta A_0 = (\mathbf{x}_a^1(t_{S-1}) - \bar{\mathbf{x}}_a^*(t_{S-1}), \dots, \mathbf{x}_a^N(t_{S-1}) - \bar{\mathbf{x}}_a^*(t_{S-1}))$.

[25] Equations (23) and (24) are used to drive next assimilation cycle, which indicates that the initial condition is perturbed only once throughout the whole assimilation in this new scheme formulation.

[26] Assimilated soil moisture content obtained from pass 1 (the state assimilation pass, Figure 1) is then passed into pass 2 (the parameter optimization pass) for parameter calibration in the same assimilation cycle. The cost function for pass 2 can be defined as follows:

$$F = \sum_{i=0}^m \left[\left(T_{b,est}^{h,V} - T_{b,obs}^{h,V} \right)^2 + \left(T_{b,est}^{l,V} - T_{b,obs}^{l,V} \right)^2 \right], \quad (25)$$

where the subscripts obs and est denote the observed and modeled values, respectively. The parameters (S , Q_0 , b') are optimized in pass 2. The SCE-UA global minimization method [Duan *et al.*, 1993] is adopted to search for the optimal values of the parameters. To minimize the effects of the initial values on the final optimized results, we assign the initial values of the parameters randomly in their value ranges at the start of each assimilation time window. The final optimized values are the averages of all the optimized values from each assimilation cycle during the parameter calibration phase. Once the parameters are optimized through the parameter calibration phase, the parameter optimization pass is turned off.

3. Numerical Experiments

[27] In this section, the new dual-pass variational assimilation framework is implemented and evaluated through a case study at a reference site located in Inner Mongolia.

3.1. Observational Data

[28] As shown in Figure 2, the reference site is centered at (112.5°E, 40.5°N) in Inner Mongolia. This site covers a flat area of about 0.65° latitude \times 0.65° longitude in a semiarid grassland, where three automated stations (i.e., ZhuoZiShan, LiangChen, and FengZhen) for soil hydrology were deployed. At these stations, soil moisture content was measured for three layers from 0 to 10 cm, 10 to 20 cm, and 40 to 50 cm on the 8th, 18th, and 28th days of each month from 8 March to 8 November 2006. This observed volumetric soil moisture data set is suitable for evaluating data assimilation as it is independence of the microwave brightness temperature data.

[29] A common issue is how to compare in situ point measurements with assimilated soil moisture averaged over a grid box of satellite observations. Soil moisture measured at a single point is often representative merely on a limited spatial scale, depending on heterogeneity of soil properties, land cover, and atmospheric conditions. Figure 3 shows that

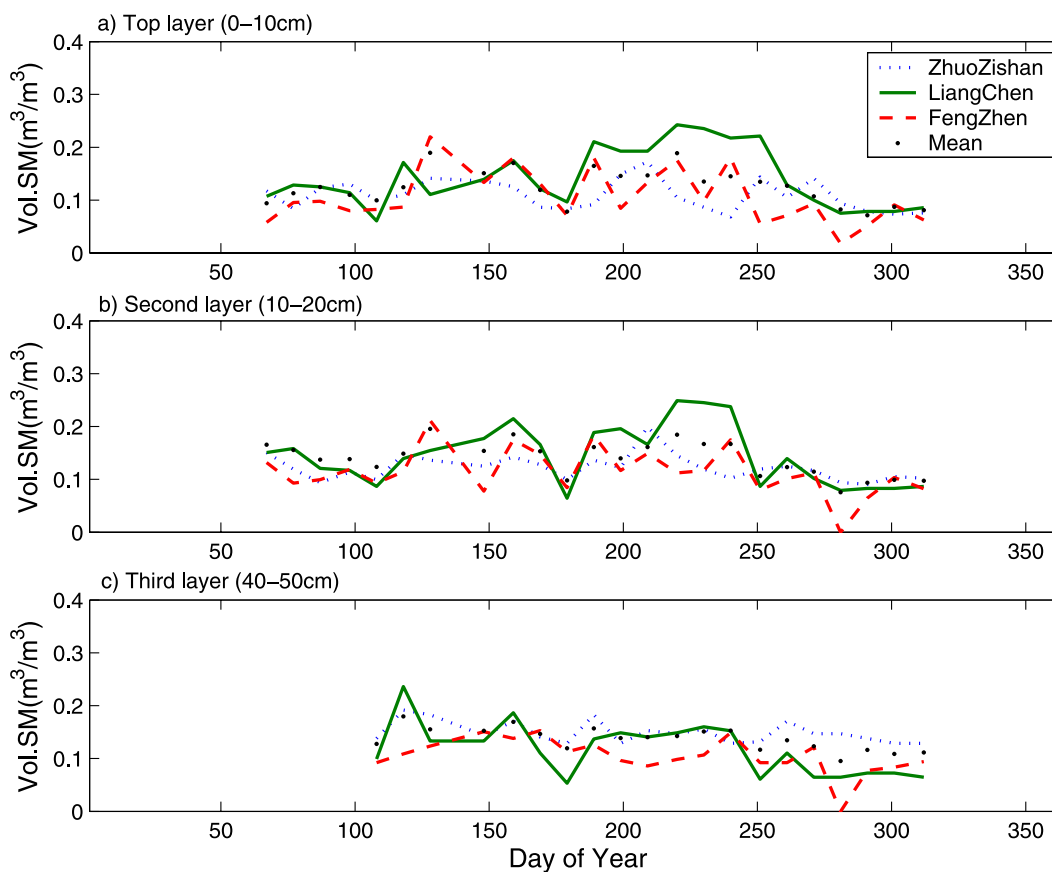


Figure 3. Time series of daily volumetric soil moisture (meters cubed per meters cubed) for the (a) top (0–10 cm), (b) second (10–20 cm), and (c) third (40–50 cm) layers from observations at the three stations (ZhuoZishan, LiangChen, and FengZhen) and their averages, respectively.

time series of daily volumetric soil moisture from observations at the three stations differ significantly even though they are close to each other. To reduce the scale mismatch, we used the arithmetic mean of the observed soil moisture contents from the three stations as a proxy for the mean state of this reference site, which approximately matches the collocated grid box ($\approx 0.6^\circ$ latitude \times 0.6° longitude centered at 112.48°E , 40.49°N) from the satellite observations.

[30] The AMSR-E satellite brightness temperature data (daily) from 1 January to 31 December 2006 used in this study was downloaded from <https://wist.echo.nasa.gov/api/> (more information about the AMSR-E satellite data can be found at <http://www.ghcc.msfc.nasa.gov/AMSR/>).

3.2. Numerical Experiments

[31] We ran the CLM3, a comprehensive land surface model described in detail by *Oleson et al.* [2004] and *Dickinson et al.* [2006], with observation-based atmospheric forcing from *Qian et al.* [2006] and *Shi* [2008]. These simulations were described elsewhere [*Tian et al.*, 2007; *Shi*, 2008] and they were used in this case study to derive the infiltration, ground temperature, surface soil temperature and canopy temperature (Figure 4) for forcing the dual-pass variational assimilation framework. In this sense, we coupled our assimilation framework with the CLM3 partially.

[32] The CLM3 simulation was first forced with the 3-hourly forcing data from 1973 to 2004 extracted from the global forcing data set created by *Qian et al.* [2006] during a

50-year spin-up run from the start-up file of *Qian et al.* [2006] to obtain an equilibrium state. From this state, the CLM3 was forced by a high-resolution (hourly and 0.2° latitude \times 0.2° longitude) data set over China created by *Shi* [2008] from 1 January to 31 December 2006 to obtain 1-year time series of simulated infiltration (= precipitation – evapotranspiration – surface runoff – interception by vegetation), ground temperature and vegetation temperature (Figure 4) for driving the dual-pass variational assimilation framework. This high-resolution forcing data set was developed by integrating observed precipitation, air temperature and other fields from about 2000 automated weather stations in the China Meteorological Administration (CMA) operational network. This high-resolution forcing data set has been successfully used in land data assimilation [*Shi*, 2008]. The assimilation time window in this study is 1 day (48 time steps) and the sampling frequency of the satellite observed brightness temperature is once per day. We used the 3 months from June to August 2006 as the parameter calibration phase to calibrate the three parameters (S , Q_0 , b') for the Q-h model to avoid snow cover at this reference site during the calibration period. Of course, longer calibration phase is more suitable for a reliable and robust parameter value. However, in this study, the length of the calibration phase is limited by the observations available. In fact, we first use the whole year (not only the 3 months) observations for calibrating. Its results are very similar with those using the 3 months (not shown). This conclusion is not

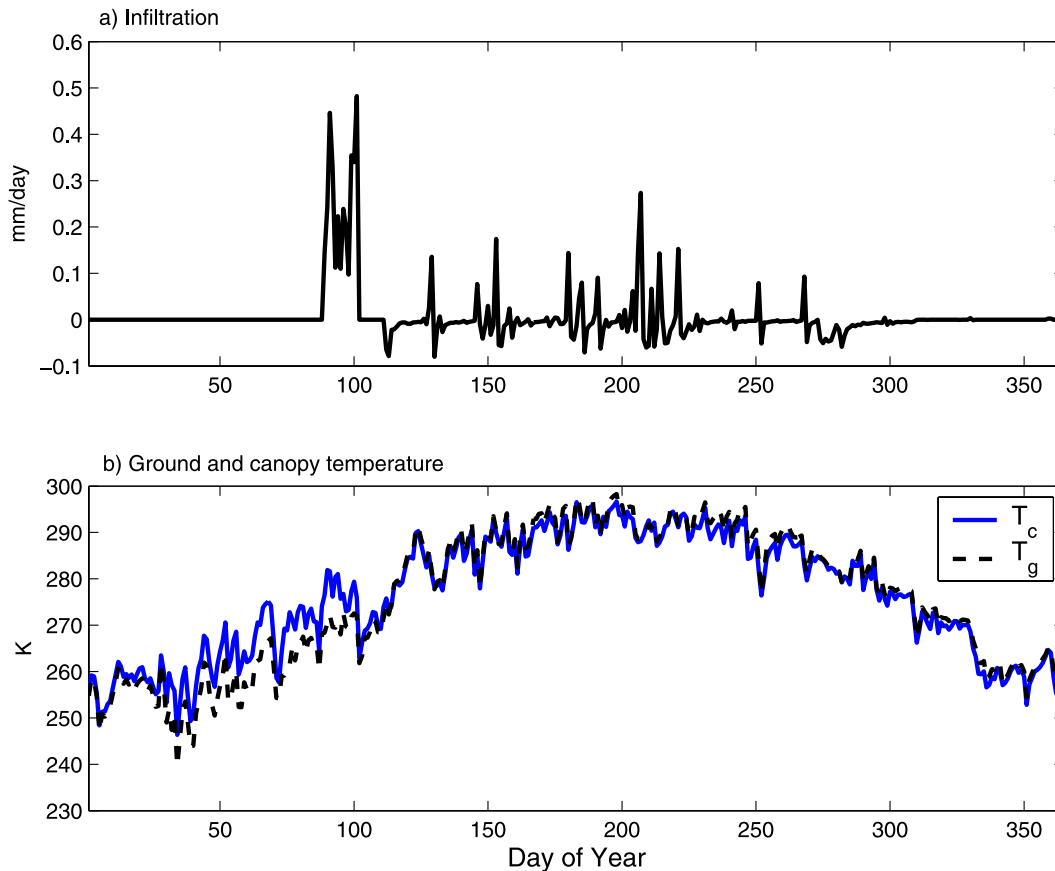


Figure 4. Time series of CLM3-simulated infiltration, ground temperature, and canopy temperature at this reference site from 1 January to 31 December 2006.

absolute and case-dependent. Anyway, more observations and longer calibration phase are needed in the future.

3.3. Experimental Results

[33] Figure 5a shows the time series brightness temperatures observed at two frequencies (6.9 and 18.7 GHz) from vertical (V) and horizontal (H) polarization that were used in this assimilation experiment. Figures 5b–5d show the time series of assimilated using vertical and horizontal polarization measurements, simulated and observed daily soil moisture content in the top layer (0–10 cm), the second layer (10–20 cm) and the third layer (40–50 cm) from 1 January to 31 December 2006. The assimilated daily soil moisture using vertical polarization measurements is capable of reproducing the temporal evolution of observed soil moisture, in terms of both its amplitude and seasonal phase. The correlation with the observed soil moisture is 0.59 for the assimilated (using V polarization measurements) and 0.01 for the simulated soil moisture in the three topsoil layers. It is encouraging that, to a considerable extent, this soil moisture improvement further propagates to lower layers where satellite observations are unavailable (Figures 5c and 5d). This results in considerable improvement to the whole modeled soil moisture profiles (Figures 5b–5d). Certainly, the deeper the soil layer depth, the less the improvement (Figures 5c and 5d). This is expected because the observational information is only available for the skin layer. On the contrary, Figures 5b–5d show that the CLM3-simulated soil

moisture deviates from (underestimates) the observations significantly since day 110, even though it performs fairly well during the initial stage from day 1 to day 110 or so. The final forcing to drive the 1-D soil water model is the infiltration, which is calculated by the CLM3 and heavily affected by the atmospheric forcing including the precipitation and the temperature data. The errors in the atmospheric forcing probably make the simulated soil moisture underestimates the observations significantly since day 110. According to *Fujii* [2005], the H polarization is more sensitive to vegetation coverage while vertical polarization is not so. Vegetation affects the H polarization so much that little useful information can be extracted from the H polarization measurements for assimilating soil moisture. As a result, the assimilated daily soil moisture using the H polarization measurements has little temporal variability and cannot catch the observed variations in observed soil moisture (Figures 5b–5d).

[34] To investigate the impacts of the ensemble size of the En4DVar method on the assimilated results, we designed another group of experiments to test its sensitivity. Three ensemble numbers are adopted: $N = 100$, 60, and 30, respectively. Figure 6 shows the time series of observed, CLM3-simulated, and three assimilated (Ass1 for $N = 100$, Ass2 for $N = 60$, and Ass3 for $N = 30$, respectively) daily soil moisture content in the top layer (0–10 cm) and the second layer (10–20 cm). It is obvious that the two assimilated (Ass1 and Ass2) soil moisture time series are

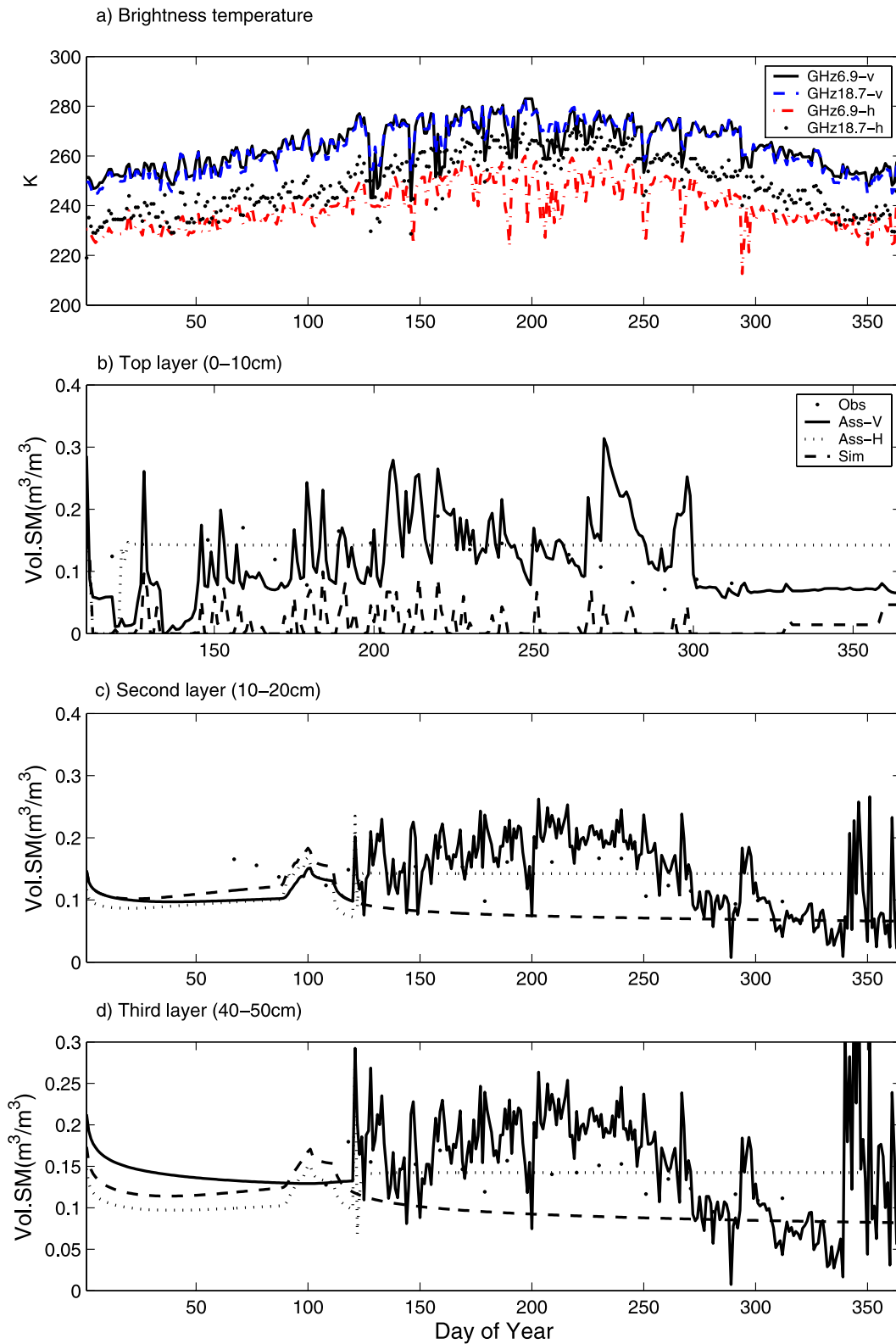


Figure 5. (a) Time series of daily Advanced Microwave Scanning Radiometer–EOS microwave brightness temperature (from vertical polarization and horizontal polarization) from 1 January to 31 December 2006, and the daily volumetric soil moisture (in meters cubed per meters cubed) for the (b) top (0–10 cm), (c) second (10–20 cm), and (d) third (40–50 cm) layers from observations (dots), the CLM3 simulation (long-dashed line), and the dual-pass assimilation framework using vertical polarization measurements (solid line) and using horizontal polarization measurements (short-dashed line) at the study site.

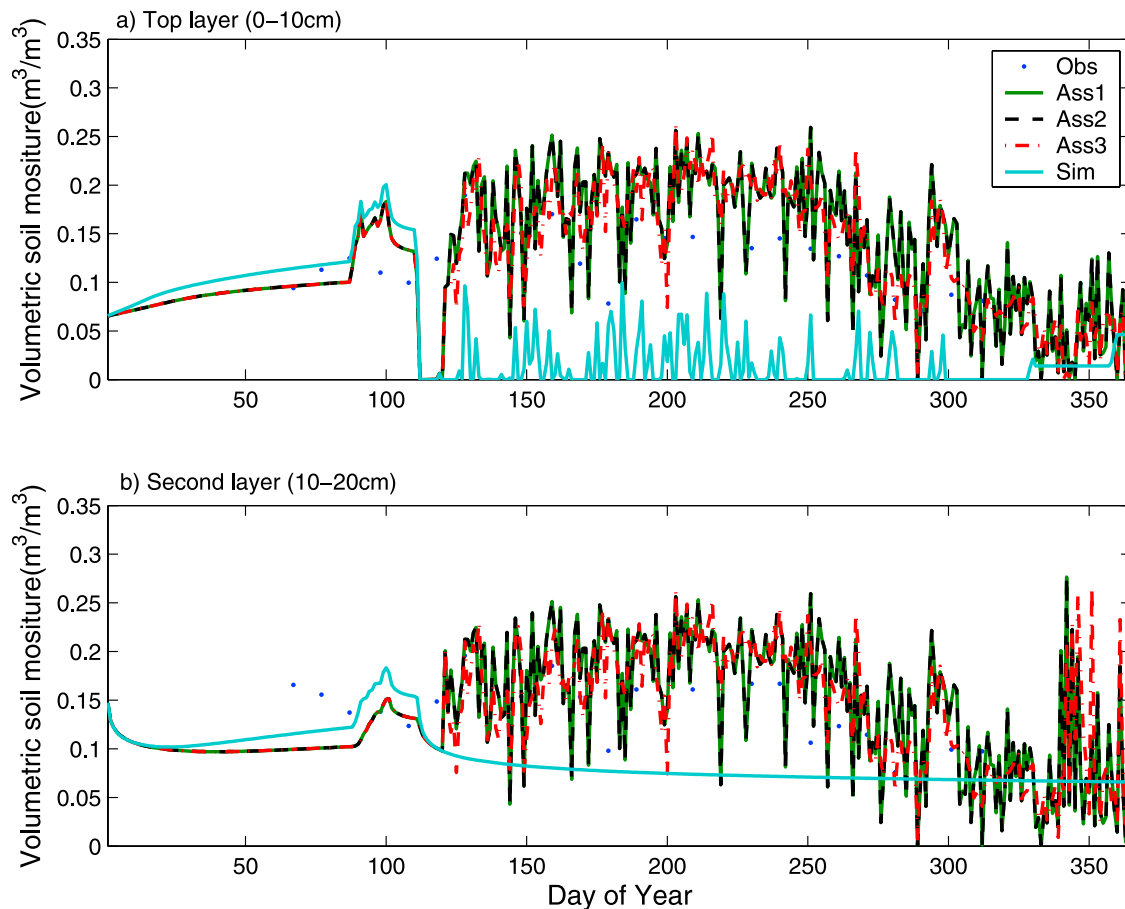


Figure 6. Time series of daily volumetric soil moisture (in meters cubed per meters cubed) from 1 January to 31 December 2006 from observations (dots), the CLM3 simulation, and the dual-pass assimilation framework with the ensemble sizes $N = 100$ (Ass1), $N = 60$ (Ass2), and $N = 30$ (Ass3) for the (a) top (0–10 cm) and (b) second (10–20 cm) soil layers.

almost the same; however, the assimilated soil moisture with $N = 30$ (Ass3) is somewhat different with the other two. We also tested another larger ensemble size $N = 200$ (not shown), whose assimilated results are similar to Ass1 and Ass2. On the basis of these results, we conclude that 60 ensembles of random perturbations are probably enough in our framework.

4. Summary and Concluding Remarks

[35] To overcome the difficulties in determining the optimal parameters needed for a radiative transfer model (RTM), which acts as the observational operator in a land data assimilation system, we have designed a dual-pass assimilation (DP-En4DVar) framework to optimize the model state (volumetric soil moisture content) and model parameters simultaneously using the gridded AMSR-E satellite brightness temperature data. This algorithm embeds a dual-pass (the state assimilation pass and the parameter optimization pass) optimization technique based on an ensemble-based four-dimensional variational assimilation method and a shuffled complex evolution approach (SCE-UA). The SCE-UA method optimizes the parameters using observational information, thereby leading to improved simulations. This algorithm is implemented differently in

two phases: the parameter calibration phase and the pure assimilation phase. Both passes are applied in each assimilation time window during the parameter calibration phase. However, only the state assimilation pass is used in the pure assimilation phase after the parameters are determined during the parameter calibration phase.

[36] Numerical experiments for a site in northern China for 2006 performed with this framework partially coupled with the NCAR CLM3 show that this dual-pass variational assimilation framework performs reasonably well and better than the pure CLM3 simulations forced with observed precipitation and other atmospheric forcing. It has the ability to reproduce the soil moisture evolution, with the amplitude and seasonal phase comparable to observed. It is also encouraging that the improvement in the assimilated soil moisture for the top 10-cm layer also propagates to lower layers, even though the satellite brightness temperature observations are available only for the skin soil layer. We also investigate the impacts of ensemble size N on the assimilated results and found that $N = 60$ is already enough to accomplish this assimilation task well.

[37] It should be pointed out that we did not incorporate this dual-pass variational assimilation framework into the Community Land Model (CLM3) fully in this study. How to develop an integrated global land data assimilation

system using satellite microwave data based on this assimilation framework and the CLM3 or other land models is a still nontrivial task for future research.

[38] **Acknowledgments.** We thank two anonymous reviewers for helpful comments. The code of microwave radiative transfer model was developed by Toshio Koike and Xin Li, with minor revisions by one author (Kun Yang). This study was supported by the National Natural Science Foundation of China (grant 40705035), the National High Technology Research and Development Program of China (grants 2009AA12Z129 and 2007AA12Z144), the Knowledge Innovation Project of the Chinese Academy of Sciences (grants KZCX2-YW-217 and KZCX2-YW-126-2), and the National Basic Research Program (grant 2005CB321703). The National Center for Atmospheric Research is sponsored by the U.S. National Science Foundation.

References

- Beezley, J. D., and J. Mandel (2008), Morphing ensemble Kalman filters, *Tellus, Ser. A*, *60*, 131–140.
- Chahine, T. M. (1992), The hydrological cycle and its influence on climate, *Nature*, *359*, 373–380, doi:10.1038/359373a0.
- Crow, W. T., and E. F. Wood (2003), The assimilation of remotely sensed soil brightness temperature imagery into a land surface model using ensemble Kalman filtering: A case study based on ESTAR measurements during SGP97, *Adv. Water Resour.*, *26*, 137–149, doi:10.1016/S0309-1708(02)00088-X.
- Darcy, H. (1856), *Les Fontaines Publiques de la Ville de Dijon*, Dalmont, Paris.
- Dickinson, R. E., K. W. Oleson, G. B. Bonan, F. Hoffman, P. Thornton, M. Vertenstein, Z. L. Yang, and X. Zeng (2006), The Community Land Model and its climate statistics as a component of the Community Climate System Model, *J. Clim.*, *19*, 2302–2324, doi:10.1175/JCLI3742.1.
- Dirmeyer, P. A., A. J. Dolman, and N. Sato (1999), The pilot phase of the Global Soil Wetness Project, *Bull. Am. Meteorol. Soc.*, *80*, 851–878, doi:10.1175/1520-0477(1999)080<0851:TPPOTG>2.0.CO;2.
- Dobson, M. C., F. T. Ulaby, M. T. Halikainen, and M. A. El-Rayes (1985), Microwave dielectric behavior of wet soil—part II: Dielectric mixing models, *IEEE Trans. Geosci. Remote Sens.*, *GE-23*, 35–46, doi:10.1109/TGRS.1985.289498.
- Duan, Q., V. K. Gupta, and S. Sorooshian (1993), A shuffled complex evolution approach for effective and efficient global minimization, *J. Optim. Theory Appl.*, *76*, 501–521, doi:10.1007/BF00939380.
- Entekhabi, D., J. F. Galantowicz, and E. G. Njoku (1994), Solving the inverse problem for soil moisture and temperature profiles by sequential assimilation of multifrequency remotely sensed observation, *IEEE Trans. Geosci. Remote Sens.*, *32*, 438–448, doi:10.1109/36.295058.
- Evensen, G. (1994), Sequential data assimilation with a nonlinear quasi-geostrophic model using Monte Carlo methods to forecast error statistics, *J. Geophys. Res.*, *99*, 10,143–10,162.
- Evensen, G. (2003), The ensemble Kalman filter: Theoretical formulation and practical implementation, *Ocean Dyn.*, *53*, 343–367, doi:10.1007/s10236-003-0036-9.
- Fujii, H. (2005), Development of a microwave radiative transfer model for vegetated land surface based on comprehensive in-situ observations, PhD diss., Univ. of Tokyo.
- Houser, P. R., W. J. Shuttleworth, J. S. Famiglietti, H. V. Gupta, K. H. Syed, and D. C. Goodrich (1998), Integration of soil moisture remote sensing and hydrologic modeling using data assimilation, *Water Resour. Res.*, *34*, 3405–3420, doi:10.1029/1998WR900001.
- Jackson, T. J. (1993), Measuring surface soil moisture using passive microwave remote sensing, *Hydrol. Process.*, *7*, 139–152, doi:10.1002/hyp.3360070205.
- Jackson, T. J., and T. J. Schmugge (1991), Vegetation effects on the microwave emission of soils, *Remote Sens. Environ.*, *36*, 203–212, doi:10.1016/0034-4257(91)90057-D.
- Kalnay, E., H. Li, T. Miyoshi, S. C. Yang, and J. Ballabrera-Poy (2007), 4-D-Var or ensemble Kalman filter?, *Tellus, Ser. A*, *59*, 758–773, doi:10.1111/j.1600-0870.2007.00261.x.
- Ly, H. V., and H. T. Tran (2001), Modeling and control of physical processes using proper orthogonal decomposition, *Math. Comput. Model.*, *33*, 223–236, doi:10.1016/S0895-7177(00)00240-5.
- Ly, H. V., and H. T. Tran (2002), Proper orthogonal decomposition for flow calculations and optimal control in a horizontal CVD reactor, *Q. Appl. Math.*, *60*, 631–656.
- Mitchell, K. E., et al. (2004), The multi-institution North American Land Data Assimilation System (NLDAS): Utilizing multiple GCM products and partners in a continental distributed hydrological modeling system, *J. Geophys. Res.*, *109*, D07S90, doi:10.1029/2003JD003823.
- Moradkhani, H., K.-L. Hsu, H. Gupta, and S. Sorooshian (2005a), Uncertainty assessment of hydrologic model states and parameters: Sequential data assimilation using the particle filter, *Water Resour. Res.*, *41*, W05012, doi:10.1029/2004WR003604.
- Moradkhani, H. S., S. Sorooshian, H. V. Gupta, and P. Houser (2005b), Dual state-parameter estimation of hydrologic model using ensemble Kalman filter, *Adv. Water Resour.*, *28*, 135–147, doi:10.1016/j.advwatres.2004.09.002.
- Nijssen, B., R. Schnur, and D. P. Lettenmaier (2001), Global retrospective estimation of soil moisture using the variable infiltration capacity land surface model, 1980–93, *J. Clim.*, *14*, 1790–1808, doi:10.1175/1520-0442(2001)014<1790:GREOSM>2.0.CO;2.
- Njoku, E. G., and D. Entekhabi (1996), Passive microwave remote sensing of soil moisture, *J. Hydrol. Amsterdam*, *184*, 101–129, doi:10.1016/0022-1694(95)02970-2.
- Njoku, E. G., T. J. Jackson, V. Lakshmi, T. K. Chan, and S. V. Nghiem (2003), Soil moisture retrieval from AMSR-E, *IEEE Trans. Geosci. Remote Sens.*, *41*, 215–229, doi:10.1109/TGRS.2002.808243.
- Oleson, K. W., et al. (2004), Technical description of the community land model (CLM), *Rep. NCAR/TN-461+STR*, 186 pp., Natl. Cent. for Atmos. Res., Boulder, Colo.
- Owe, M., R. de Jeu, and J. Walker (2001), A methodology for surface soil moisture and vegetation optical depth retrieval using the microwave polarization difference index, *IEEE Trans. Geosci. Remote Sens.*, *39*, 1643–1654, doi:10.1109/36.942542.
- Paloscia, S., and P. Pampaloni (1988), Microwave polarization index for monitoring vegetation growth, *IEEE Trans. Geosci. Remote Sens.*, *26*, 617–621, doi:10.1109/36.7687.
- Paloscia, S., G. Macelloni, E. Santi, and T. Koike (2001), A multifrequency algorithm for the retrieval of soil moisture on a large scale using microwave data from SMMR and SSM/I satellites, *IEEE Trans. Geosci. Remote Sens.*, *39*, 1655–1661, doi:10.1109/36.942543.
- Qian, T., A. Dai, K. E. Trenberth, and K. W. Oleson (2006), Simulation of global land surface conditions from 1948 to 2004. Part I: Forcing data and evaluations, *J. Hydrometeorol.*, *7*, 953–975, doi:10.1175/JHM540.1.
- Reichle, R. H., and D. Entekhabi (2001), Downscaling of radio brightness measurements for soil moisture estimation: A four-dimensional variational data assimilation approach, *Water Resour. Res.*, *37*, 2353–2364.
- Reichle, R. H., D. Entekhabi, and D. B. McLaughlin (2001), Downscaling of radio brightness measurements for soil moisture estimation: A four-dimensional variational data assimilation approach, *Water Resour. Res.*, *37*, 2353–2364, doi:10.1029/2001WR000475.
- Reichle, R. H., D. B. McLaughlin, and D. Entekhabi (2002a), Hydrologic data assimilation with the ensemble Kalman filter, *Mon. Weather Rev.*, *130*, 103–114, doi:10.1175/1520-0493(2002)130<0103:HDAWTE>2.0.CO;2.
- Reichle, R. H., J. P. Walker, R. D. Koster, and P. R. Houser (2002b), Extended versus ensemble Kalman filtering for land data assimilation, *J. Hydrometeorol.*, *3*, 728–740, doi:10.1175/1525-7541(2002)003<0728:EVEKFF>2.0.CO;2.
- Sellers, P. J., D. A. Randall, G. J. Collatz, J. A. Berry, C. B. Field, D. A. Dazlich, C. Zhang, G. D. Collelo, and L. Bounoua (1996), A revised land surface parameterization (SIB2) for atmospheric GCMs. Part I: Model formulation, *J. Clim.*, *9*, 676–705, doi:10.1175/1520-0442(1996)009<0676:ARLSPF>2.0.CO;2.
- Seuffert, G., H. Wilker, P. Viterbo, J. F. Mahfouf, M. Drusch, and J. C. Calvet (2003), Soil moisture analysis combining screen-level parameters and microwave brightness temperature: A test with field data, *Geophys. Res. Lett.*, *30*(10), 1498, doi:10.1029/2003GL017128.
- Seuffert, G., H. Wilker, P. Viterbo, M. Drusch, and J. F. Mahfouf (2004), The usage of screen-level parameters and microwave brightness temperature for soil moisture analysis, *J. Hydrometeorol.*, *5*, 516–531, doi:10.1175/1525-7541(2004)005<0516:TUOSPA>2.0.CO;2.
- Sheffield, J., and E. F. Wood (2008), Global trends and variability in soil moisture and drought characteristics, 1950–2000, from observation-driven simulations of the terrestrial hydrologic cycle, *J. Clim.*, *21*, 432–458, doi:10.1175/2007JCLI1822.1.
- Shi, C. X. (2008), A study on soil moisture remote sensing data assimilation based on ensemble Kalman filter (EnKF) (in Chinese), Ph.D. diss., 177 pp., Inst. of Atmos. Phys., Chin. Acad. of Sci., Beijing.
- Shi, J. C., J. Wang, A. Y. Hsu, P. E. O'Neill, and E. T. Engman (1997), Estimation of bare surface soil moisture and surface roughness parameter using L-band SAR image data, *IEEE Trans. Geosci. Remote Sens.*, *35*, 1254–1266, doi:10.1109/36.628792.
- Shi, J. C., L. Jiang, L. Zhang, K. S. Chen, J. P. Wigeron, and A. Chanzy (2005), A parameterized multifrequency-polarization surface emission model, *IEEE Trans. Geosci. Remote Sens.*, *43*, 2831–2841, doi:10.1109/TGRS.2005.857902.
- Tian, X., and Z. Xie (2008), A land surface soil moisture data assimilation framework in consideration of the model subgrid-scale heterogeneity and

- soil water thawing and freezing, *Sci. China*, *51*, 992–1000, doi:10.1007/s11430-008-0069-5.
- Tian, X., A. Dai, D. Yang, and Z. Xie (2007), Effects of precipitation-bias corrections on surface hydrology over northern latitudes, *J. Geophys. Res.*, *112*, D14101, doi:10.1029/2007JD008420.
- Tian, X., Z. Xie, and A. Dai (2008a), An ensemble-based explicit four-dimensional variational assimilation method, *J. Geophys. Res.*, *113*, D21124, doi:10.1029/2008JD010358.
- Tian, X., Z. Xie, and A. Dai (2008b), A land surface soil moisture data assimilation system based on the dual-UKF method and the Community Land Model, *J. Geophys. Res.*, *113*, D14127, doi:10.1029/2007JD009650.
- Ulaby, F. T., R. K. Moore, and A. K. Fung (1986), *Microwave Remote Sensing: Active and Passive*, vol. 3, *From Theory to Applications*, Artech House, Norwood, Mass.
- Vrugt, J. A., C. G. H. Diks, H. V. Gupta, W. Bouten, and J. M. Verstraten (2005), Improved treatment of uncertainty in hydrologic modeling: Combining the strengths of global optimization and data assimilation, *Water Resour. Res.*, *41*, W01017, doi:10.1029/2004WR003059.
- Walker, J. P., G. R. Willgoose, and J. D. Kalma (2001), One-dimensional soil moisture profile retrieval by assimilation near-surface observations: A comparison of retrieval algorithms, *Adv. Water Resour.*, *24*, 631–650, doi:10.1016/S0309-1708(00)00043-9.
- Wang, J. R., and B. J. Choudhury (1981), Remote sensing of soil moisture content cover bare fields at 1.4GHz frequency, *J. Geophys. Res.*, *86*, 5277–5282, doi:10.1029/JC086iC06p05277.
- Wegmuller, U., and C. Matzler (1999), Rough bare soil reflectivity model, *IEEE Trans. Geosci. Remote Sens.*, *37*, 1391–1395, doi:10.1109/36.763303.
- Wen, J., Z. Su, and Y. Ma (2003), Determination of land surface temperature and soil moisture from Tropic Rainfall Measuring Mission/Microwave Imager remote sensing data, *J. Geophys. Res.*, *108*(D2), 4038, doi:10.1029/2002JD002176.
- Wigneron, J. P., J. C. Calvet, T. Pellarin, A. A. Van de Griend, M. Berger, and P. Ferrazzoli (2003), Retrieving near-surface soil moisture from microwave radiometric observations: Current status and future plans, *Remote Sens. Environ.*, *85*, 489–506, doi:10.1016/S0034-4257(03)00051-8.
- Yang, K., T. Watanabe, T. Koike, X. Li, H. Fujii, K. Tamagam, Y. Ma, and H. Ishikawa (2007a), An auto-calibration system to assimilate AMSR-E data into a land surface model for estimating soil moisture and surface energy budget, *J. Meteorol. Soc. Jpn.*, *85A*, 229–242, doi:10.2151/jmsj.85A.229.
- Yang, K., T. Watanabe, T. Koike, X. Li, H. Fujii, K. Tamagam, Y. Ma, and H. Ishikawa (2007b), Auto-calibration system developed to assimilate AMSR-E data into a land surface model for estimating soil moisture and the surface energy budget, *J. Meteorol. Soc. Jpn.*, *85A*, 229–242, doi:10.2151/jmsj.85A.229.
- Zhang, S. W., H. R. Li, W. D. Zhang, C. J. Qiu, and X. Li (2006), Estimating the soil moisture profile by assimilating near-surface observations with the ensemble Kalman filter (EnKF), *Adv. Atmos. Sci.*, *20*, 845–848.

F. Chen, B. Jia, X. Tian, and Z. Xie, ICCES, Institute of Atmospheric Physics, Chinese Academy of Sciences, Beijing 100029, China. (tianxj@mail.iap.ac.cn)

A. Dai, National Center for Atmospheric Research, P.O. Box 3000, Boulder, CO 80307, USA.

C. Shi, National Satellite Meteorological Center, China Meteorological Administration, Beijing 100081, China.

K. Yang, Institute of Tibetan Plateau Research Chinese Academy of Sciences, Beijing 100085, China.